

PHYSICAL REVIEW C

NUCLEAR PHYSICS

THIRD SERIES, VOLUME 43, NUMBER 6

JUNE 1991

RAPID COMMUNICATIONS

The Rapid Communications section is intended for the accelerated publication of important new results. Manuscripts submitted to this section are given priority in handling in the editorial office and in production. A Rapid Communication in Physical Review C may be no longer than five printed pages and must be accompanied by an abstract. Page proofs are sent to authors.

Superdeformation in $^{198,196}\text{Pb}$

T. F. Wang, A. Kuhnert, J. A. Becker, E. A. Henry, and S. W. Yates*
Lawrence Livermore National Laboratory, Livermore, California 94550

M. J. Brinkman and J. A. Cizewski
Rutgers University, New Brunswick, New Jersey 08903

F. A. Azaiez,[†] M. A. Deleplanque, R. M. Diamond, J. E. Draper,[‡] W. H. Kelly,[§] W. Korten,
A. O. Macchiavelli, E. Rubel,[‡] and F. S. Stephens
Lawrence Berkeley National Laboratory, Berkeley, California 94720

(Received 14 February 1991)

A weakly populated rotational band with energy spacings characteristic of superdeformation has been found in the reaction $^{154}\text{Sm}(^{48}\text{Ca},xn)$ at $E(^{48}\text{Ca})=205$ MeV. This band has seven transitions with an average γ -ray energy spacing of approximately 42 keV. It is assigned to ^{198}Pb on the basis of the excitation-function results. We also confirm the isotopic assignment of a previously reported superdeformed (SD) band in ^{196}Pb via the cross bombardments $^{176}\text{Yb}(^{26}\text{Mg},xn)$ and $^{176}\text{Yb}(^{24}\text{Mg},xn)$. Three SD bands have now been identified in the Pb isotopes with neutron numbers 112, 114, and 116.

Three-dimensional Hartree-Fock calculations of Bonche *et al.*¹ and Girod *et al.*² (who employed an effective two-body interaction with pairing), as well as a cranked Strutinsky calculation of Chasman,³ all predict well-developed secondary minima in nuclear energy surfaces throughout the $A \sim 194$ mass region, suggesting the presence of superdeformed (SD) nuclear shapes. These predictions have been verified experimentally in a number of Hg (Ref. 4), Tl (Refs. 5 and 6), and Pb (Refs. 7 and 8) nuclei. There are now approximately 25 SD bands observed in 12 nuclei in this region. These SD nuclei show similar moments of inertia, identical transition energies, and quantized alignment. Our experiments are motivated by the desire to understand these new phenomena associated with superdeformation. We report here results from our continuing experimental work in the Pb isotopes: (1) a new SD band in ^{198}Pb , and (2) confirmation of a previous⁷ tentative isotopic assignment for a SD band in ^{196}Pb .

Experiments were carried out at the Lawrence Berkeley

Laboratory 88-Inch Cyclotron using HERA. HERA is an array of 20 Compton-suppressed Ge detectors together with a 4π , 40-element bismuth germanate inner ball. ^{198}Pb was populated via the $^{154}\text{Sm}(^{48}\text{Ca},4n)$ reaction at two incident energies, $E(^{48}\text{Ca})=205$ and 210 MeV. The ^{154}Sm target was made of three stacked $500 \mu\text{g}/\text{cm}^2$ foils. ^{196}Pb was studied by bombarding a ^{176}Yb target with two Mg isotopes: ^{24}Mg at $E(^{24}\text{Mg})=122$ MeV and ^{26}Mg at $E(^{26}\text{Mg})=135$ MeV. These energies were chosen to maximize the population of ^{196}Pb via the $4n$ and $6n$ evaporation channels, respectively. The ^{176}Yb target was composed of three stacked (450 , 450 , and $700 \mu\text{g}/\text{cm}^2$) foils. Doubly-coincident (twofold) Ge events were recorded, along with sum energy (H) and multiplicity (K) information from the inner ball, if at least six inner-ball detectors were triggered. Coincidence events between three or more Ge detectors were always recorded (with H and K information). In the ^{198}Pb study, ~ 280 million coincidence events were stored at each energy. For the ^{196}Pb

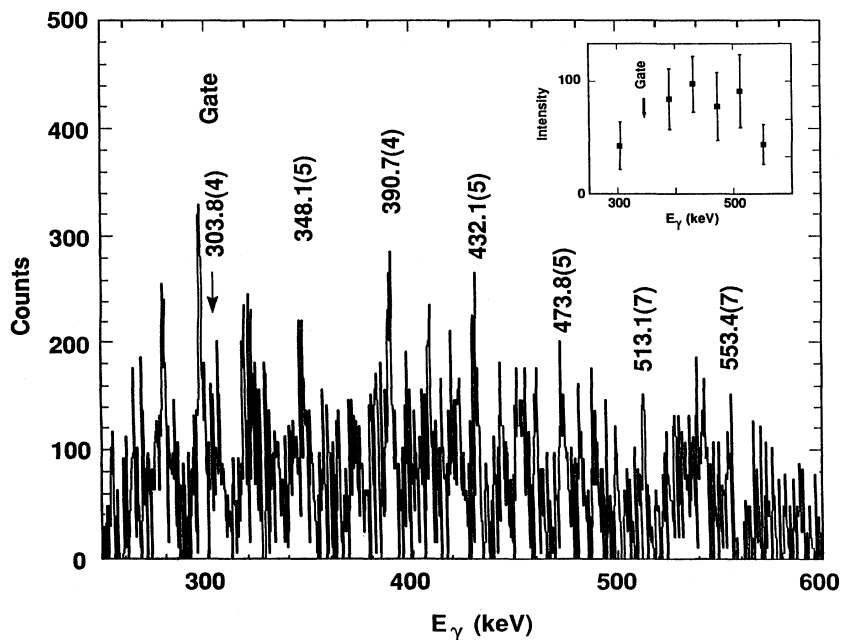


FIG. 1. Single-gated coincidence spectrum for the SD band in ^{198}Pb ; transition energies with errors are shown. The intensity pattern of the SD band gated on the 348.1-keV transition is illustrated in the upper right corner.

study, ~ 130 million and ~ 400 million coincidences were stored at $E(^{24}\text{Mg}) = 126$ MeV and $E(^{26}\text{Mg}) = 135$ MeV, respectively. In each instance, $\sim 80\%$ of the total recorded events were twofold coincidences.

Analysis of the ^{198}Pb data was done with conditions $H \geq 4.0$ MeV and $K \geq 8$. Figure 1 shows the energy spectrum and the intensity pattern of the SD band observed in the $^{154}\text{Sm}(^{48}\text{Ca}, xn)$ reaction at $E(^{48}\text{Ca}) = 205$ MeV. This band consists of seven transitions and is populated at $\sim 1\%$ of the total ^{198}Pb yield. The γ -ray energy difference between two adjacent transitions, ΔE_γ , decreases gradually from ~ 44 keV for the lowest-energy transitions to ~ 40 keV at the highest-energy transitions. The change in ΔE_γ per transition with increasing E_γ is the smallest among the SD bands so far found in Hg and Pb. The intensity ratios [the intensity obtained at $E(^{48}\text{Ca}) = 205$ MeV to that at $E(^{48}\text{Ca}) = 210$ MeV] of (i) the SD band, (ii) the high-spin states in ^{198}Pb , and (iii) the high-spin states in ^{197}Pb are summarized in Table I. There is no difference between the $K \geq 8$ and $K \geq 11$ results. The

TABLE I. The ratio of the intensity [normalized with respect to the corresponding total double-coincidence events; two different multiplicity conditions ($K \geq 8$ and $K \geq 11$) were selected] obtained at $E(^{48}\text{Ca}) = 205$ MeV to the intensity at $E(^{48}\text{Ca}) = 210$ MeV for (i) the SD band observed in the $^{154}\text{Sm}(^{48}\text{Ca}, xn)$ reaction, and (ii) the high-spin states in ^{198}Pb , and (iii) the high-spin states in ^{197}Pb .

	$K \geq 8$	$K \geq 11$
SD	2.5(9)	2.3(10)
^{198}Pb	1.9(2)	1.8(2)
^{197}Pb	0.8(1)	0.8(1)

number of events with $K \geq 11$ is $\sim 40\%$ of the number with $K \geq 8$. The SD band appears to have the same (within errors) excitation-function behavior as the high-spin states in ^{198}Pb . We, therefore, assign this SD band to ^{198}Pb . Coincidences between SD band members and transitions between known states below the 12^+ ($\tau = 240$ ns) isomer⁹ were not observed.

Figure 2(a) shows an 11-transition SD band observed in the $^{176}\text{Yb}(^{26}\text{Mg}, xn)$ reaction at $E(^{26}\text{Mg}) = 135$ MeV. Analysis was done with conditions $H \geq 3.25$ MeV and $K \geq 8$. This band was previously found⁷ in the $^{176}\text{Yb}(^{24}\text{Mg}, xn)$ reaction at $E(^{24}\text{Mg}) = 122$ MeV. Data from the latter reaction are shown in Fig. 2(b), along with the intensity pattern of the band. ^{196}Pb is the only common nucleus populated in these two reactions and, therefore, we unambiguously assign this band to ^{196}Pb . For this band ΔE_γ decreases gradually from ~ 44 to ~ 36 keV as E_γ increases from 215 to 620 keV. No known low-lying transition between states below the 12^+ ($\tau = 265$ ns) isomer¹⁰ in ^{196}Pb was found in coincidence with SD band members. No meaningful intensity pattern can be obtained from the data at $E(^{26}\text{Mg}) = 135$ MeV. The spectral peaks of the SD band are more prominent in the spectrum obtained at $E(^{24}\text{Mg}) = 122$ MeV than in the spectrum obtained at $E(^{26}\text{Mg}) = 135$ MeV, although the intensity ratio of the 959-keV ($14^+ \rightarrow 12^+$) transition¹⁰ in ^{196}Pb normalized to the total double-coincidence events at $E(^{26}\text{Mg}) = 135$ MeV to that at $E(^{24}\text{Mg}) = 122$ MeV is 0.86(2). This may be due to the population mechanism of the SD band or background produced by the other evaporation channels and fission at the higher incident energy.

The spin assignments of the members of these bands were obtained from least squares fits to the expression

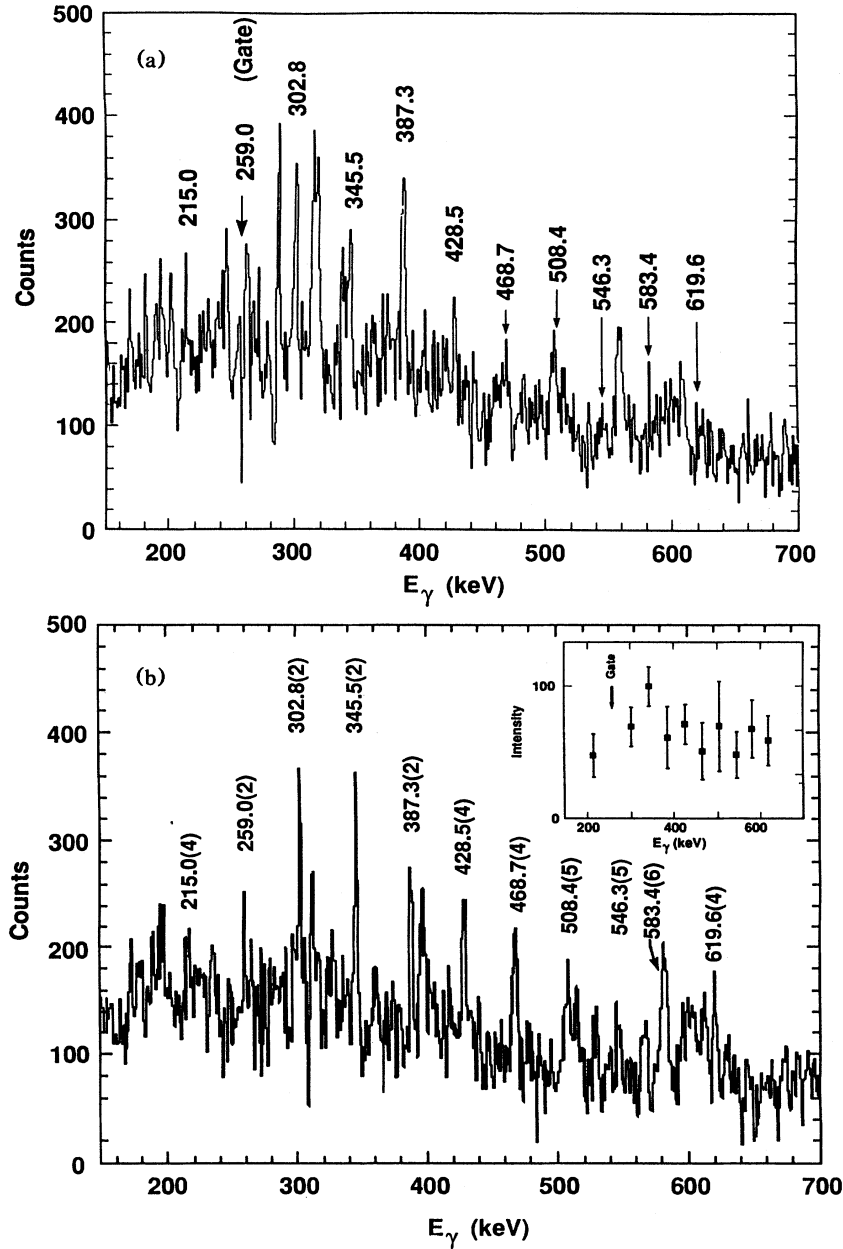


FIG. 2. (a) Spectrum for the ^{196}Pb SD band (obtained from gating on the 259.0-keV γ ray) observed in the $^{176}\text{Yb}(^{26}\text{Mg}, xn)$ reaction at $E(^{26}\text{Mg}) = 135$ MeV. (b) The same band was found in the $^{176}\text{Yb}(^{24}\text{Mg}, xn)$ reaction at $E(^{24}\text{Mg}) = 122$ MeV; the spectrum was obtained from summing the 215.0-keV, 259.0-keV, and 508.4-keV gates. The intensity pattern obtained from the 259.0-keV gate is also shown.

($\hbar = 1$):

$$I + \frac{1}{2} = 2\alpha\omega + \frac{4}{3}\beta\omega^3. \quad (1)$$

With the choice $\omega = dE/dI = E_\gamma/2$, I is the intermediate spin in the transition $I+1 \rightarrow I-1$ (see also Refs. 11 and 12). The $^{198,198}\text{Pb}$ data do not have sufficient statistics for making directional correlation analysis, and we made a reasonable assumption that these cascade γ rays of the SD band have multipolarity $L=2$. There are three free parameters in the fit: I_f (the spin of the lowest band member) and the inertial parameters α and β . All seven

transitions were used in the fit for ^{198}Pb , and only the nine lowest-energy transitions were used for ^{196}Pb . Results are summarized in Table II. The 303.8-keV γ ray in ^{198}Pb is assigned as $I_i \rightarrow I_f = 14 \rightarrow 12$, and the 215-keV γ ray in ^{196}Pb corresponds to an $I_i \rightarrow I_f = 10 \rightarrow 8$ transition. In the ^{198}Pb spin assignment, we use the fact that the level spin of an even-even nucleus is integer.

Figure 3 shows $\mathcal{J}^{(2)}$, the dynamic moment of inertia, for the SD bands in ^{198}Pb and ^{196}Pb , as a function of $(\hbar\omega)^2$. Lines through the data points are obtained with the parameters for integer values I_f in Table II. The $\mathcal{J}^{(2)}$ values

TABLE II. Least-squares parameters from a fit of measured transition energies to $I + \frac{1}{2} = 2\alpha\omega + \frac{4}{3}\beta\omega^3$ (see text). The errors are statistical only, and when $\chi^2/\nu < 1$, the error represents the uncertainty: $(\chi^2/\nu)^{1/2}\sigma$. The second row for a given nucleus represents the fit done with a fixed integer value I_f .

AZ	E_γ (keV)	α ($\times 10^{-2}$) (keV $^{-1}$)	β ($\times 10^{-8}$) (keV $^{-3}$)	I_f
^{194}Pb	169.7(2)	4.408(24)	8.17(43)	6.02(5)
		4.398(4)	8.33(16)	6
^{196}Pb	215.0(4)	4.344(20)	6.28(27)	7.94(5)
		4.369(2)	5.95(11)	8
^{198}Pb	303.8(4)	4.265(65)	5.87(74)	11.74(17)
		4.361(7)	4.83(21)	12

of the SD band^{7,8} in ^{194}Pb are included in Fig. 3 for comparison. While many of the even-even nuclei have similar $\mathcal{J}^{(2)}$, the $\mathcal{J}^{(2)}(^{198}\text{Pb})$ and $\mathcal{J}^{(2)}(^{196}\text{Pb})$ are different than $\mathcal{J}^{(2)}(^{194}\text{Pb})$, although all three nuclei have almost the same moment of inertia, 2α . The change in $\mathcal{J}^{(2)}$ per transition decreases with increasing neutron number. A possible interpretation is that the pairing does not change as much with frequency in $^{198,196}\text{Pb}$ as in ^{194}Pb . The alignment¹³ of the $^{198,196}\text{Pb}$ SD bands with increasing $\hbar\omega$ does not saturate at a quantized value (i.e., integer or half-integer) with respect to the ^{192}Hg (or ^{193}Tl) reference SD band (see Refs. 13 and 6 for the prescription and details), in contrast to the many other SD bands in this region. Furthermore, the SD bands in $^{198,196}\text{Pb}$ do not show quantized alignment with respect to any reported SD band in the $A = 194$ region.

An important result of this experiment is that the region of superdeformation is extended to $N = 116$. All calculations predict well-defined secondary minima in ^{194}Pb , ^{196}Pb , and ^{198}Pb ; however, the excitation energy of the second well increases with increasing neutron number. For example, Bonche *et al.*¹ predict that the depth of the second minimum increases from 1.73 MeV for ^{194}Pb to 2.59 MeV for ^{198}Pb while the excitation energy increases from 4.86 MeV to 8.28 MeV. The calculation of Chasman³ includes angular momentum. He predicts that the second minimum in ^{198}Pb at $I = 40$ has depth ~ 3.4 MeV and excitation energy ~ 4.2 MeV above yrast. Based on Chasman's calculation, our observation of the SD band in ^{198}Pb is surprising and suggests that the population mechanism is not yet well understood.

Bonche *et al.*¹⁴ have discussed the termination of the SD cascade and the decay to the first well states. They made fully self-consistent generator coordinate method calculations on a basis of quadrupole constrained Hartree-Fock plus BCS wave functions. In-band *versus* out-of-band quadrupole decay was evaluated, and they find (i) the depopulation of the SD band takes place at approxi-

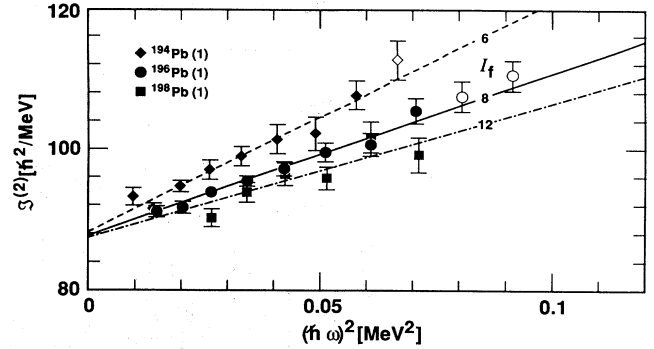


FIG. 3. The dynamic moment of inertia $\mathcal{J}^{(2)}$ of the SD band in ^{194}Pb , ^{196}Pb , and ^{198}Pb as a function of $(\hbar\omega)^2$. The lines are calculated from the parameters α and β obtained with integer values of I_f . The solid symbols indicate the transitions which were used in the fits.

mately the correct spin value in Hg and Pb and (ii) the decay of the SD band occurs in 1-2 transitions. Also, the predicted trend of the cascade termination with A is consistent with experimental results. They predict that the SD band depopulates at $I = 12$ in ^{198}Pb , as we observed in our experiment.

The behavior of the inertial parameter α with mass A is interesting (see Table II): α is constant within 1% as A changes from 194 to 198, while the rigid body moment of inertia ($\propto A^{5/3}$) would give a 3% change. Krieger *et al.*¹⁵ have calculated the moment of inertia and the electric quadrupole moment for the even-even Pb isotopes with A between 190 and 218. The predicted moment of inertia show a 3% increase between $A = 194$ and 198, and a flat plateau which changes $\sim 1.5\%$ (per four mass units) in the mass region $A = 198-210$.

In summary, we have extended the region of superdeformation to $N = 116$. ^{198}Pb is the heaviest nucleus in this mass region where the superdeformation is known. Further experiments, e.g., a search for SD bands in heavier Pb nuclei ($^{199,200}\text{Pb}$) and lighter Pb nuclei ($^{191,192}\text{Pb}$), as well as finding linking transitions are essential to understanding the physics associated with superdeformation.

The authors thank M. S. Weiss, P. Bonche, S. J. Krieger, and R. R. Chasman for fruitful discussions. We also thank the LBL 88-Inch Cyclotron operating crew for flawless operation. We acknowledge R. A. Belshe, M. Lee, and D. R. Manatt for their help in the data acquisition during the experiment. This work was supported in part by the Department of Energy, under Contract No. W-7405-ENG-48 (LLNL), in part by the U.S. Department of Energy under Contract No. DE-AC03-76SF-00098 (LBL) and by the National Science Foundation (Rutgers).

- *Permanent address: University of Kentucky, Lexington, KY 40506.
- †Permanent address: Centre d'Etudes Nucléaires de Bordeaux-Gradignan, Institut National de Physique Nucléaire et de Physique des Particules, Le haut-vigneau 33170, Gradignan, France.
- ‡Permanent address: University of California, Davis, CA 95616.
- §Permanent address: Iowa State University, Ames, IA 50011.
- ¹P. Bonche *et al.*, Nucl. Phys. A **500**, 308 (1989). Further calculations (P. Bonche *et al.*, LLNL Report No. UCRL-JC-105461, 1990), predict secondary minima from Gd through Actinides.
- ²M. Girod *et al.*, Phys. Rev. Lett. **62**, 2452 (1989).
- ³R. R. Chasman, Phys. Lett. B **219**, 227 (1989).
- ⁴See, for example, E. A. Henry *et al.*, Z. Phys. A **335**, 325 (1990); R. V. F. Janssens *et al.*, Nucl. Phys. A **520**, 75c (1990), and references therein.
- ⁵P. B. Fernandez *et al.*, Nucl. Phys. A **517**, 386 (1990).
- ⁶F. Azaiez *et al.*, Phys. Rev. Lett. **66**, 1030 (1991).
- ⁷M. J. Brinkman *et al.*, Z. Phys. A **336**, 115 (1990).
- ⁸K. Theine *et al.*, Z. Phys. A **336**, 113 (1990).
- ⁹K. Honkanen *et al.*, Nucl. Phys. A **451**, 141 (1986).
- ¹⁰J. J. van Ruyven *et al.*, Nucl. Phys. A **449**, 579 (1986).
- ¹¹J. A. Becker *et al.*, Nucl. Phys. A **520**, 187c (1990).
- ¹²J. E. Draper *et al.*, Phys. Rev. C **42**, R1791 (1990).
- ¹³F. Stephens *et al.*, Phys. Rev. Lett. **65**, 301 (1990); **64**, 2623 (1990).
- ¹⁴P. Bonche, J. Dobaczewski, H. Flocard, P. H. Heenen, S. J. Krieger, J. Meyer, and M. S. Weiss, Nucl. Phys. A **519**, 509 (1990).
- ¹⁵S. J. Krieger *et al.* (unpublished).